J Mater Sci: Mater Med (2009) 20:S235–S241
DOI 10.1007/s10856-008-3548-5

Role of size scale of ZnO nanoparticles and microparticles on toxicity toward bacteria and osteoblast cancer cells

Shantikumar Nair · Abhilash Sasidharan · V. V. Divya Rani · Deepthy Menon · Seema Nair · K. Manzoor · Satish Raina

Received: 20 November 2007 / Accepted: 18 July 2008 / Published online: 21 August 2008

Abstract The specific role of size scale, surface capping, and aspect ratio of zinc oxide (ZnO) particles on toxicity toward prokaryotic and eukaryotic cells was investigated. ZnO nano and microparticles of controlled size and morphology were synthesized by wet chemical methods. Cytotoxicity toward mammalian cells was studied using a human osteoblast cancer cell line and antibacterial activity using Gram-negative bacteria (*Escherichia coli)* as well as using Gram-positive bacteria (*Staphylococcus aureus)*. Scanning electron microscopy (SEM) was conducted to characterize any visual features of the biocidal action of ZnO. We observed that antibacterial activity increased with reduction in particle size. Toxicity toward the human cancer cell line was considerably higher than previously observed by other researchers on the corresponding primary cells, suggesting selective toxicity of the ZnO to cancer cells. Surface capping was also found to profoundly influence the toxicity of ZnO nanoparticles toward the cancer cell line, with the toxicity of starch-capped ZnO being the lowest. Our results are found to be consistent with a membrane-related mechanism for nanoparticle toxicity toward microbes.

S. Nair (✉) · A. Sasidharan · V. V. Divya Rani · D. Menon · S. Nair · K. Manzoor
Amrita Center for Nanosciences, Amrita Vishwa Vidyapeetham, Kochi 682 026, Kerala, India
e-mail: shantinair@aims.amrita.edu

S. Raina
Institute of Molecular Medicine, Amrita Institute of Medical Sciences, Kochi 682 026, Kerala, India

1 Introduction

Zinc oxide (ZnO) is currently being investigated as an antibacterial agent in both microscale and nanoscale formulations. Results have indicated that ZnO nanoparticles show antibacterial activity [1–11] apparently greater than for microparticles [1]. While the exact mechanisms of the antibacterial action have not yet been clearly elucidated, suggested mechanisms include, the role of reactive oxygen species (ROS) generated on the surface of the particles [2–4], zinc ion release [5], membrane dysfunction [5, 6], and nanoparticle internalization [7]. The role of ROS needs further study because the influence of light on antibacterial effect related to ROS production is not conclusive. Although one study reported substantial inhibition of bacterial growth under dark conditions, another showed significant antibacterial effect under dark conditions, both studies being on *Escherichia coli*. Furthermore, there is no effect of illumination on the antibacterial effect in certain Gram-positive bacteria [8]. Nevertheless, the excellent study by Sawai et al. [4] clearly showing that ROS concentrations increased with the ZnO content of slurries makes this mechanism worthy of further detailed evaluations. With regard to the role of cell membrane versus cell internalization, one transmission electron microscopy study showed that many particles of 10–14 nm ZnO were internalized [7] after overnight exposure, but membrane damage was also observed. The effect of particle size on internalization of ZnO is not known. Another aspect of relevance to completed studies is the role of the medium in which the exposures are carried out. ZnO can be processed through diethylene glycol (DEG) or aqueous routes. In the former case, DEG can cause damage to bacterial membranes [7], which complicates the interpretation of the role of ZnO.

A systematic study of the influence of size scale and surface chemistry is critical to an understanding of the toxicity mechanisms. There is only one previous study of the influence of particle size on the antibacterial activity of ZnO [1]. In this study, reagent grade ZnO powder was obtained over a size range of 100–800 nm by ball milling. The study reported increasing toxicity as the size decreased, but in all cases significant toxicity toward *E. coli* was observed above a concentration of 12 μM of ZnO.

An important aspect of the use of ZnO as antibacterial agent is the requirement that the particles are not toxic to human cells. Published studies showed that ZnO nanoparticles were toxic to T-cells above 5 mM concentration [9] and toxic to neuroblastoma cells above 1.2 mM [10]. Thus, it appears that toxicity to the neuro cells were greater than toward bacteria, while the opposite was true for T-cells. A study by Colon et al. [11] showed that nanophase ZnO actually improved normal osteoblast function, indicating non-toxicity. Clearly the type of cell in question is important when considering human cell toxicity of ZnO.

In this study, we specifically explore the question of size scale and surface capping (chemistry) on the balance between bacterial and human cell toxicity. ZnO was synthesized with a well-defined range of sizes using wet chemical methods in an aqueous base and using specific capping agents that provide approximately monolayer coverage on ZnO particles. Non-aqueous bases, such as DEG, were avoided to preclude the complicating effects of DEG on antibacterial activity and human cell toxicity. Both Gram positive and Gram negative bacteria were considered for antibacterial studies. Osteoblast cells were selected for toxicity studies because of their significance in bone tissue engineering applications. However, our study explores the influence of ZnO on an osteoblast cancer cell line (MG-63). Since ZnO improved the functions of primary osteoblasts, we were interested in whether a cancer cell line of the same cell type provided a similar result. A potential application of ZnO nanoparticles as an antibacterial and an anticancer agent would provide new opportunities for this material in nanomedicine.

2 Materials and methods

2.1 Materials

The wild type *E. coli* (W3110) was obtained from *E. coli* genetic stock center (Yale) and *Staphylococcus aureus* (ATCC 25923) was from the Microbiology Lab of Amrita Institute of Medical Sciences, Kochi, India. Luria-Bertani (LB) medium was used for growing and maintaining *E. coli,* while Brain Heart Infusion (BHI) broth (Himedia Laboratories, Mumbai, India) was used for *S. aureus*. The human osteoblast cancer cell line (MG-63) was provided by National Chemical Laboratory, Pune, India. The cells were cultured in Minimal Essential Medium (MEM, Sigma-Aldrich, USA) with 10% fetal bovine serum (FBS, Sigma-Aldrich, USA).

2.2 Synthesis of ZnO nanoparticles

2.2.1 Equiaxed ZnO nanoparticles

All the chemicals used for the synthesis of nanoparticles were of reagent grade and procured from Sigma Aldrich, USA. Spherical nanoparticles of ZnO were synthesized by mixing 0.1 M of zinc acetate dihydrate and 0.025–0.2 M of NaOH in methanol. The reaction mixture was vigorously stirred for 20 min at ambient temperature with poly ethylene glycol (PEG) as a surfactant during synthesis. The amount of added PEG per unit gram of ZnO was selected so as to get an approximate monolayer coverage over 40 nm size nanoparticles. A rough calculation will show that this corresponds approximately to 0.1 g of PEG per gram of ZnO. There are reports that PEG molecules link with ZnO through hydrogen bonding [12]. In the present case, PEG molecules with average molecular weight 8000 have a chain length of ~87 nm. The average surface area of a molecule of this length is about 19 nm^2. The surface area of a ZnO particle of size 40 nm is about 500 nm^2, so that about 25 molecules of PEG is required to provide full surface coverage. This corresponds to about 0.1 g PEG per gram of ZnO. In order to remove the byproducts (sodium acetate) the precipitate was washed several times with ethanol, de-ionized water and then re-dispersed in de-ionized water by ultrasonication.

2.2.2 ZnO nanorods

The ZnO nanorods were synthesized according to the method documented in reference [13] with slight modification. Typically, 0.5 M Zinc nitrate hexahydrate was dissolved in 0.5% soluble starch solution and 1 M NaOH was dissolved in deionized water. Under constant stirring, the zinc nitrate solution was added slowly (drop wise for 30 min) to NaOH solution which was maintained at ~70°C. After 2 h reaction time, the white precipitate deposited at the bottom of the flask was collected and washed several times with absolute ethanol and distilled water. ZnO samples were obtained by centrifugation and dehydration of the precipitate in vacuum at 60–70°C and finally re-dispersed in de-ionized water by ultrasonication.

2.3 Characterization

Analytical scanning electron microscope (JEOL, model JSM-6490 LA) was used to study the size and surface morphology of ZnO nanoparticles. Crystallinity of the samples was studied using an X-ray diffractometer [Rigaku Dmax-C] fitted with a Cu-K_α source. The phase identification was carried out with the help of standard JCPDS database. A Nicomp Particle Size Analyser (Nicomp 380, Particle Sizing Systems, USA) was utilized for the particle size analysis, employing the technique of Dynamic Light Scattering. The average particle size as well as dispersion in size could be noted from this measurement.

2.4 Antibacterial activity

Escherichia coli and *S. aureus* were used as test bacteria. These bacteria were grown overnight in LB & BHI medium, respectively. Various concentrations (1–7 mM) of autoclaved ZnO particles were added to the broth, with the nanoparticles-free LB broth as the control. *E. coli* culture (100 µl) with an approximate concentration of 10^6 colony forming units per milliliter (CFU/ml) was inoculated to 10 ml media. The culture tubes containing the nanoparticles were incubated with shaking (200 rpm) in a water bath at 37°C. After 24 h, cell viability was measured by serial dilution of the culture in 10 mM $MgSO_4$, followed by plating on solid media. The viable cell number was recorded by counting the number of bacterial colonies grown on the plate multiplied by the dilution factor and expressed as CFU/ml. The surface morphology of both treated and untreated *E. coli* was studied using Scanning electron microscopy (SEM).

2.5 Cytotoxicity

Human osteoblast cancer cells (MG-63) were cultured in Minimum Essential Medium Eagle (MEM) with 10% FBS, 50 IU/ml penicillin, 50 µg/ml streptomycin, and 50 µg/ml amphotericin respectively, incubated at 37°C under a humidified atmosphere with 5% CO_2. When the cells reached confluence, cells were harvested and 5×10^4/ml cells were seeded to 96 well plates and incubated for 24 h at 37°C in 5% CO_2 atmosphere. Media containing various concentrations (1 µM, 100 µM, 500 µM, 1 mM, 3 mM, 5 mM, 7 mM) of ZnO nanoparticles were added to the 96 well plates. Triton X100 (1%) was used as positive control for toxicity and ZnO-free culture media as the negative control. The cells were then incubated with the nanoparticles for 24 h and MTT assay (Cell growth determination kit, Sigma, USA) was performed. The optical absorbance at 570 nm was recorded using microplate reader [Bio-Rad Model 680].

3 Results and discussion

3.1 Characterization of ZnO particles

The crystalline phase structure of ZnO is depicted in the XRD spectrum shown in Fig. 1. The diffraction peaks corresponding to ZnO with hexagonal-type structure XRD pattern was detected and verified with the JCPDS data file available in literature. The prominent reflections were found to match well with the standard peaks of ZnO. Figure 2 shows the SEM micrographs of PEG-capped ZnO nanoparticles, indicating uniform spherical morphology. ZnO particle size was tuned by varying NaOH concentration as depicted in Fig. 3a. Adopting this aqueous synthesis route, particle sizes were varied from 40 nm to 1.2 µm, with the same capping agent on all particle surfaces. This allowed for a systematic study of the role of size scale on toxicity. Typical DLS results of ZnO particle size distribution of 40 nm as well as 350 nm samples are shown in Fig. 3b, c, respectively. In the case where starch was used a capping agent, the shape of the particle could be controlled to obtain nano-rod structures, with an aspect ratio of about 5, as shown in Fig. 2b.

3.2 Effect of particle size and shape on toxicity

3.2.1 Antibacterial activity

Representative results of the bacterial count for various sizes (40 nm–1.2 µm) of PEG-capped ZnO particles for different concentrations (1–7 mM) are shown in Fig. 4. The results shown in Fig. 5a indicate that antibacterial activity toward *E. coli* increased as the particle size decreased from micro to the nano regime. Clearly, toxicity was observed only above 5 mM concentration levels of ZnO, with no apparent toxicity for PEG. This was consistent with the results of Yamamoto [1] except for the fact that antibacterial activity was observed only above 5 mM, as against 12 µM concentration in their report. A recent

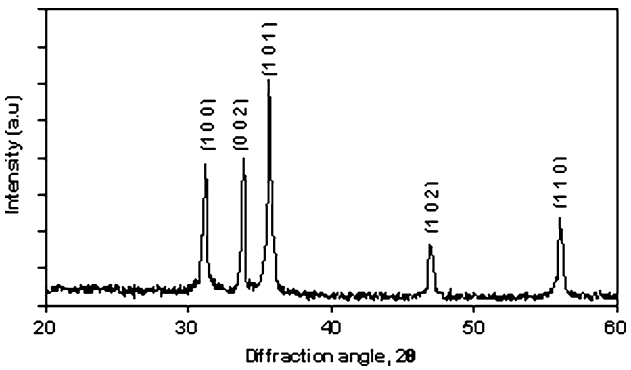

Fig. 1 X-ray diffraction pattern of synthesized zinc oxide

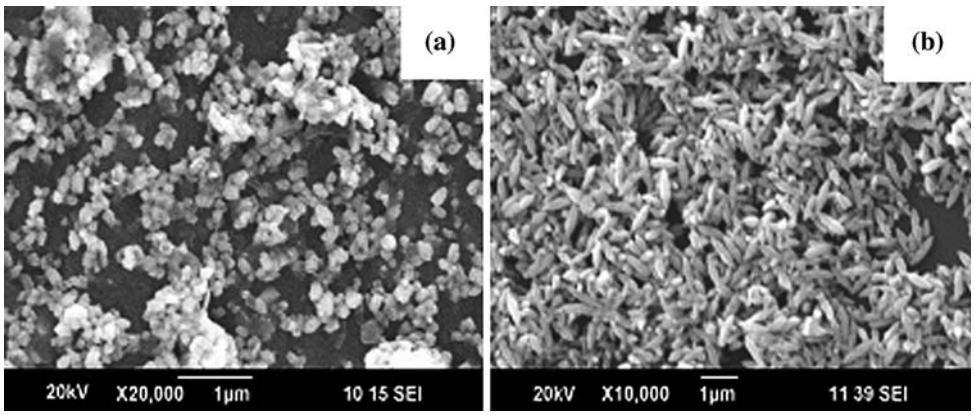

Fig. 2 Representative SEM images of ZnO nanoparticles (**a**) spherical (350 nm) and (**b**) rod shaped

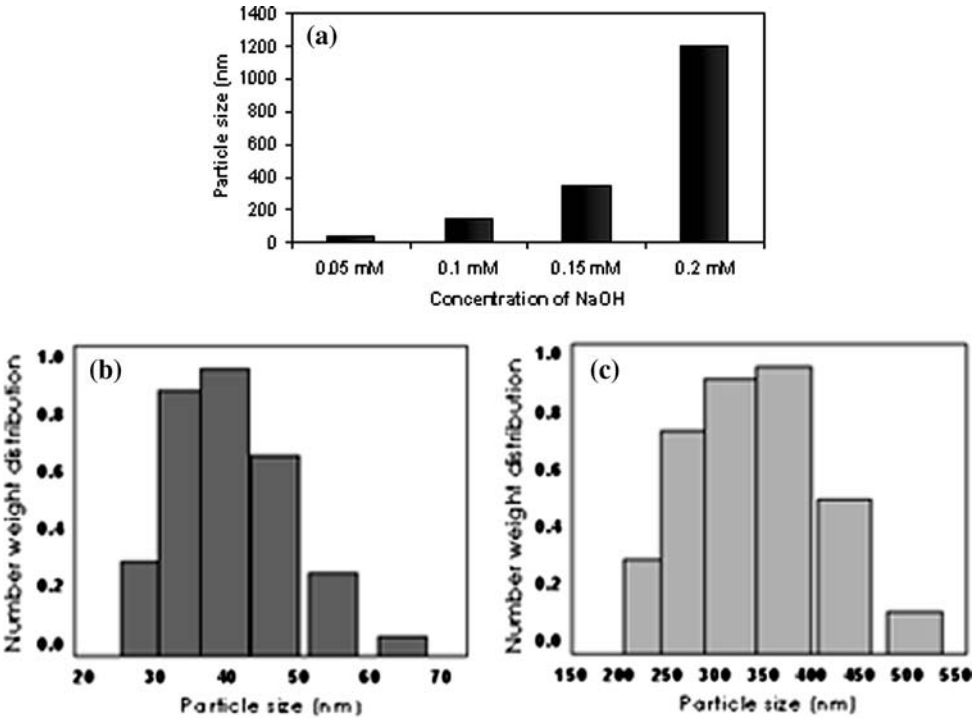

Fig. 3 (**a**) Effect of NaOH concentration on ZnO particle size. Representative plot showing particle size distribution of (**b**) 40 and (**c**) 350 nm ZnO particles

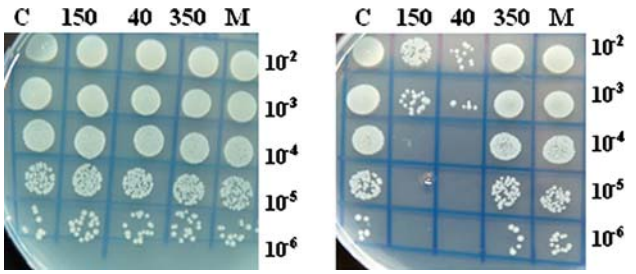

Fig. 4 *E. coli* grown on LB agar plates after incubation with different particle sizes of ZnO for two representative concentrations (1 and 7 mM). (C, control; M, micron sized ZnO)

study [14] indicated that a PEGylated PAMAM dendrimer had similar antibacterial activity when compared to a non-PEGylated dendrimer, suggesting that PEG may not play any special protective role against ZnO for bacteria. Similarly PEG encapsulated vancomycin showed the same antibacterial activity as native vancomycin [15]. The increased antibacterial activity of the ZnO particles used in Yamamoto's investigation may therefore relate to the reduced number of initial bacterial cells (10^2 CFU as against 10^6 CFU in the present study). The initial number of bacterial cells is critical in the antibacterial activity of nanoparticles, as observed in the case of silver nanoparticles [16]. With regard to the mechanism of antibacterial action of our PEG-capped ZnO, substantial loss of membrane integrity as seen by changes in cell morphology of bacterial (*E. coli*) surface was observed in the SEM analysis of the bacteria before and after ZnO exposure, as shown in Fig. 6. A recent study [17] suggests that PEG has the ability to act as a free-radical scavenger and, in our view, the PEGylated ZnO may be less susceptible to ROS

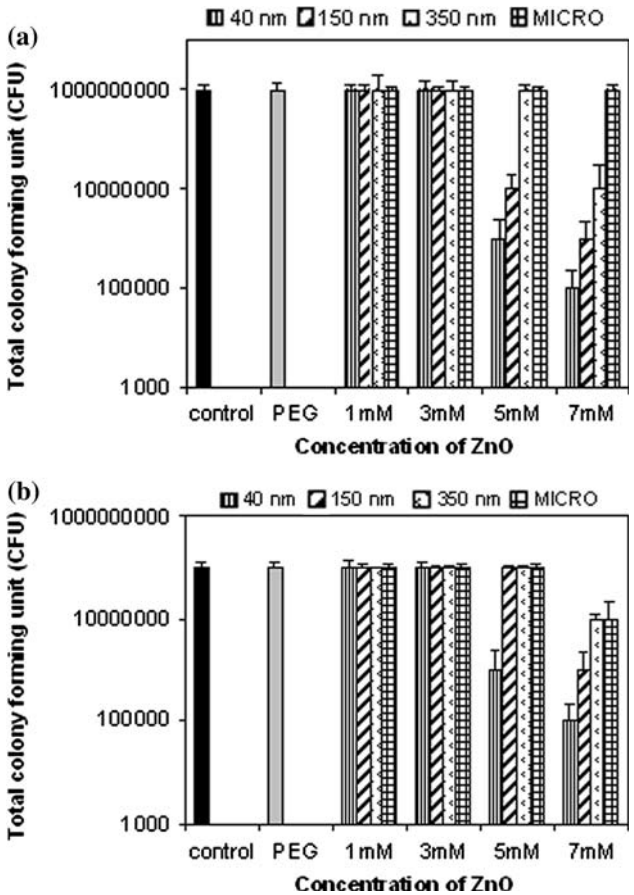

Fig. 5 Number of (**a**) *E. coli* and (**b**) *S. aureus* colonies grown on LB agar plates at different particle sizes of ZnO

damage. We propose that the relevant mechanism in our case is membrane dysfunction brought about by the interaction of ZnO with the cell membrane. This process is aided by the fact that ZnO particles, prepared in non-aqueous medium (methanol) leading to oxygen deficient (Zinc rich) surface, would exhibit a strong electrostatic interaction with the negatively charged cell membrane. This mechanism is consistent with the observed increase in antibacterial activity with decreasing size, because the smaller sized particles would be expected to have a higher surface charge because of the increased surface area per unit volume.

The proposed mechanism of action of PEGylated ZnO on *E. coli* is similar to the antibacterial action on Gram positive bacteria, *S. aureus*. However, the effect toward the Gram positive bacteria is less than that on Gram negative bacteria at the same concentration (say, 5 mM), as shown in Fig. 5b. Also, the influence of particle size on antibacterial activity toward *S. aureus* was less than that for *E. coli*. This is in contrast to the previous result using bare ZnO nanoparticles in DEG, which showed a much stronger antibacterial effect on Gram positive bacteria [7]. We believe that this difference can be due to the change in the interaction mechanisms of ZnO with the bacterial membrane. Gram positive bacteria have much thicker peptidoglycan cell wall compared to Gram negative and are likely less susceptible to ZnO induced membrane damage. However, when an ROS mechanism is active, both membranes (that for the Gram positive and for the Gram negative) are equally permeable to ROS and the susceptibility differences would be related to the intracellular events.

The antibacterial activity of starch-coated ZnO is less than PEG-capped 40 nm size ZnO for equivalent concentrations as shown by comparing Figs. 5a and 7. Only when the PEG-capped ZnO is in the micron regime does PEG-capping provide less antibacterial action than starch-capping. Thus, starch-capping appears to provide some degree of protection to bacteria from ZnO nanoparticles when compared to PEG-capping. This result is not consistent with an ROS mechanism because PEG is known to be an ROS scavenger [17]. From the standpoint of a membrane-damage mechanism there is consistency because starch has a larger number of OH groups compared to PEG and these groups can quench the surface positive charges on ZnO and thereby reduce the nanoparticle-membrane interaction.

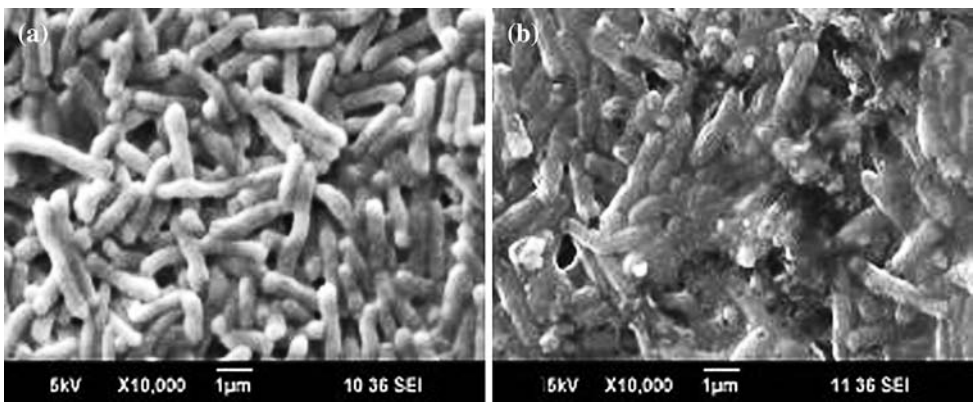

Fig. 6 SEM images of *E. coli* (**a**) before antibacterial test (**b**) after treatment

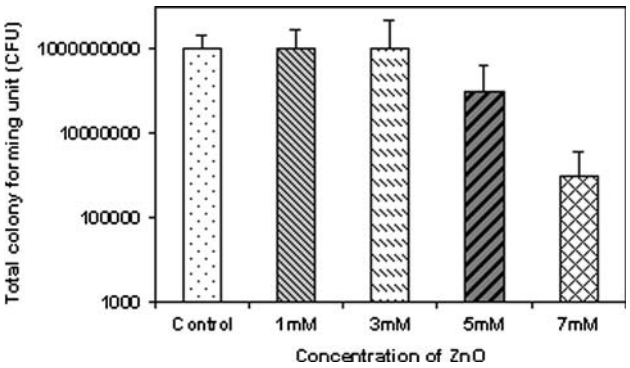

Fig. 7 Number of *E. coli* colonies grown on LB agar plates after incubation with starch-capped ZnO nanorods

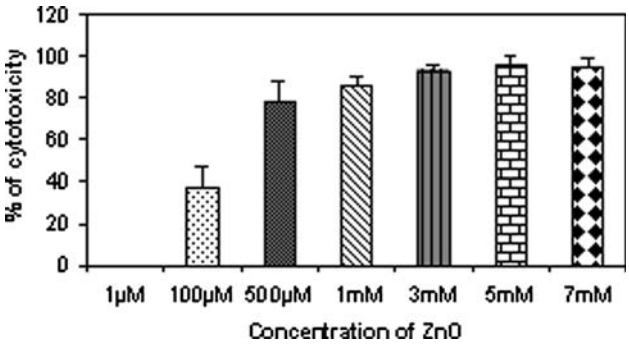

Fig. 9 Cytotoxicity of osteoblast cancer cells after 24 h exposure to ZnO nanorods

3.2.2 *Cytotoxicity*

The percentage cytotoxicity of PEG-capped ZnO on human osteoblast cancer cell line is shown in Fig. 8. It is evident that ZnO is extremely toxic to the cancer cells at all concentrations above 100 μM, as against a threshold concentration of 5 mM for bacteria. The starch coated ZnO nanorods as shown in Fig. 9, also exhibit toxicity toward the MG63 cell line. In contrast, the work by Colon et al. [11] showed an enhanced adhesion on normal human osteoblast cell line. This exciting result needs further detailed investigations. The fact that the starch or PEG coating does not abate cancer cell toxicity is also very useful since such coatings can protect the normal cells further from any potential cytotoxic effects. In the work by Colon et al. [11], compared to the polystyrene reference, ZnO nanophase was about 40% toxic compared to about 74% toxicity of the micron sized ZnO to normal osteoblasts. Thus, nanophase was friendlier than the microphase toward normal osteoblasts, whereas, in our study, the nanoparticles were more toxic to the cancer cells than the corresponding microparticles of ZnO. Our work points to the possibility that the use of suitable surface capping can reduce this inherent toxicity toward normal cells, but still maintain the high toxicity toward cancer cells. Cytotoxicity induced by nanoparticles has been attributed to a variety of mechanisms, which include, particle-induced apoptosis by upregulation of Fas on the cell membrane, membrane damage and by intracellular effects associated with particle endocytosis. The upregulation of Fas indicates a link to anticancer activity [18], which suggests that ZnO cytotoxicity may be related to enhanced membrane-mediated apoptosis. This is certainly speculative at this point and needs further careful studies, especially to explain the possible selective toxicity to cancer cells.

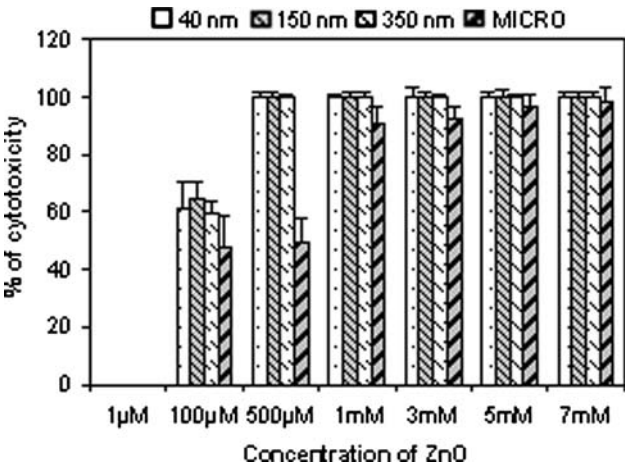

Fig. 8 Cytotoxicity of osteoblast cancer cells after 24 h exposure to ZnO particles

4 Conclusions

(1) ZnO nanoparticles that were PEG-capped were increasingly antibacterial in nature as the size was reduced from the micro to the nanoscale and for increasing concentrations. The antibacterial activity was less toward Gram positive than toward Gram negative bacteria, but the functional dependence on particle size was the same. The results suggested a membrane dysfunction mechanism for antibacterial action. Starch capping of the nanoparticles appeared to provide greater protection to bacteria possibly due to the OH-related quenching of positive charges on the ZnO nanoparticle surface. The results suggest a membrane-damage mechanism of antibacterial action in favor of an ROS model.

(2) PEG-capped nanoparticles were highly toxic to cancer cells, with a very low concentration threshold for cytotoxic action. It is hypothesized that the cytotoxicity was related to nanoparticle-enhanced apoptosis by upregulation of Fas on the cell membrane. Cytotoxicity was also found to reduce with starch capping.

Acknowledgments We are grateful to the Department of Science and Technology, Government of India for financial support through the Nanoscience and Nanotechnology (NS & NT) initiative monitored by Professor C.N.R. Rao. We are thankful to Sajin P. Ravi for SEM analysis.

References

1. O. Yamamoto, Int. J. Inorg. Mater. **3**, 643 (2001)
2. J. Sawai, E. Kawada, F. Kanou, H. Igarashi, A. Hashimoto, T. Kokugan, M. Shimizu, J. Chem. Eng. Jpn. **29**, 627 (1996)
3. J. Sawai, H. Kojima, H. Igarashi, A. Hashimoto, S. Shoji, A. Takehara, T. Sawaki, T. Kokugan, M. Shimizu, J. Chem. Eng. Jpn. **30**, 1034 (1997)
4. J. Sawai, S. Shouji, H. Igarashi, A. Hashimoto, T. Kokugan, M. Shimizu, H. Kojima, J. Ferment. Bioeng. **86**, 521 (1998)
5. Z. Yang, C. Xie, Colloids Surf B Biointerfaces **47**, 132 (2006)
6. L. Zhang, Y. Ding, M.J.W. Povey, D.W. York, J. Nanopart. Res. **9**, 479 (2007)
7. R. Brayner, R. Ferrari-Iliou, N. Brivois, S. Djediat, M.F. Benedetti, F. Fievet, Nano Lett. **6**, 866 (2006)
8. L.K. Adams, D.Y. Lyon, P.J. Alvarez, Water Res. **40**, 3527 (2006)
9. K.M. Reddy, K. Feris, J. Bell, D.G. Wingett, C. Hanley, A. Punnoose, Appl. Phy. Lett. **90**, 213902 (2007)
10. H.A. Jeng, J. Swanson, J. Enviorn. Sci. Health **41**, 2699 (2006)
11. G. Colon, B.C. Ward, T.J. Webster, J. Biomed. Mater. Res. **78**, 595 (2006)
12. C. Sheng, F. Liu, Powder Technol. **145**, 20 (2004)
13. W. Changle, O. Xueliang, C. Jianguo, W. Hongshui, T. Fatang, L. Shitao, Mater. Lett. **60**, 1828 (2006)
14. M.K. Calbretta, A. Kumar, A.M. Mcdermott, C. Cai, Biomacromolecules **8**, 1807 (2007)
15. R.B. Greenwald, H. Zhao, J. Xi, A. Martinez, J. Med. Chem. **46**, 5021 (2003)
16. S. Pal, Y.K. Tak, J.M. Song, Appl. Environ. Microbiol. **73**, 1712 (2007)
17. P. Liu-Snynder, M.P. Logan, R. Shi, D.T. Smith, R.B. Borgens, J. Exp. Biol. **210**, 1455 (2007)
18. L.B. Owen-Szcaub, Clin. Cancer Res. **7**, 1108 (2001)